

Chemical Science

Accepted Manuscript

This article can be cited before page numbers have been issued, to do this please use: E. S. Gulyaeva, E. S. Osipova, S. A. Kovalenko, O. A. Filippov, N. Belkova, L. Vendier, Y. CANAC, E. Shubina and D. A. Valyaev, *Chem. Sci.*, 2023, DOI: 10.1039/D3SC05356C.



This is an Accepted Manuscript, which has been through the Royal Society of Chemistry peer review process and has been accepted for publication.

Accepted Manuscripts are published online shortly after acceptance, before technical editing, formatting and proof reading. Using this free service, authors can make their results available to the community, in citable form, before we publish the edited article. We will replace this Accepted Manuscript with the edited and formatted Advance Article as soon as it is available.

You can find more information about Accepted Manuscripts in the [Information for Authors](#).

Please note that technical editing may introduce minor changes to the text and/or graphics, which may alter content. The journal's standard [Terms & Conditions](#) and the [Ethical guidelines](#) still apply. In no event shall the Royal Society of Chemistry be held responsible for any errors or omissions in this Accepted Manuscript or any consequences arising from the use of any information it contains.

ARTICLE

Two active species from a single metal halide precursor: a case study of highly productive Mn-catalyzed dehydrogenation of amine-boranes via intermolecular bimetallic cooperation

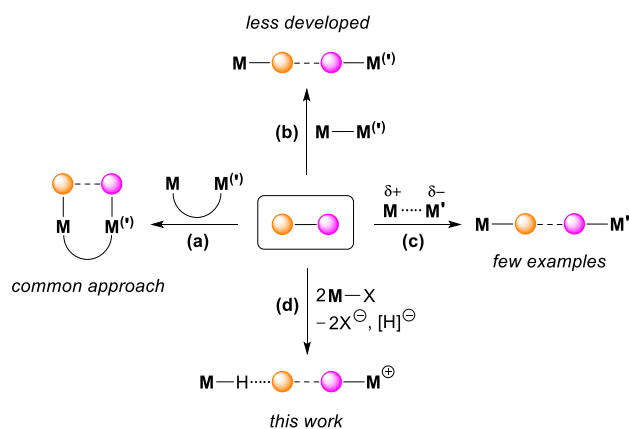
Ekaterina S. Gulyaeva,^{a,b} Elena S. Osipova,^b Sergey A. Kovalenko,^b Oleg A. Filippov,^{*b} Natalia V. Belkova,^b Laure Vendier,^a Yves Canac,^{*a} Elena S. Shubina^{*b} and Dmitry A. Valyaev^{*a}Received 00th January 20xx,
Accepted 00th January 20xx

DOI: 10.1039/x0xx00000x

Metal-metal cooperation for inert bond activation is an ubiquitous concept in coordination chemistry and catalysis. While the great majority of such transformations proceeds *via* intramolecular mode in binuclear complexes, only few examples of intermolecular small molecules activation are known to date using usually bimetallic frustrated Lewis pairs ($M^{6+}\cdots M'^{6-}$). We introduce herein an alternative approach for the intermolecular bimetallic cooperativity observed in catalytic dehydrogenation of amine-boranes, in which the concomitant activation of N–H and B–H bonds of the substrate proceeds by a synergetic action of Lewis acidic (M^+) and basic hydride ($M-H$) metal species derived from the same mononuclear complex ($M-Br$). It was also demonstrated that this system generated *in situ* from air-stable Mn(I) complex *fac*- $[(CO)_3(bis(NHC))MnBr]$ and $NaBPh_4$ shows high activity for H_2 production from several substrates (Me_2NHBH_3 , $tBuNH_2BH_3$, $MeNH_2BH_3$, NH_3BH_3) at low catalyst loading (0.1% to 50 ppm) providing outstanding efficiency for Me_2NHBH_3 (TON up to 18200) largely superior to all known 3d, *s*-, *p*-, *f*-block metal derivatives and FLPs. These results permit to take a step forward towards more extensive use of intermolecular bimetallic cooperation concept in a modern homogeneous catalysis.

Introduction

Cooperative action of two metal atoms for the activation of organic molecules often accompanied by inert bond cleavage is omnipresent for heterogeneous catalysts,¹ metalloenzymes² and related biomimetic systems.³ In coordination chemistry, these processes generally take place in the *intramolecular* mode within well-defined homo- or heterobimetallic complexes (Scheme 1, (a)), in which two metal atoms are kept in a close proximity by bridging ligand(s)³ occasionally supported by additional metal-metal interaction.⁴ Similar reactivity was also observed for binuclear derivatives with highly polarized metal-metal single bond (Scheme 1, (b)) also known as metal-only Lewis pairs (MOLPs).^{5,6} In the latter case, if inert bond of the substrate is completely cleaved two resulting monometallic species can participate in a single catalytic cycle with a synergetic effect.⁷ In a sharp contrast, *intermolecular* cooperative activation of small molecules mediated by two mononuclear transition metal species (Scheme 1, (c)) remains scarce.⁸ The most pertinent examples of such behavior deal



- ➡ Readily available manganese pre-catalyst
- ➡ No activation with strong base or UV light
- ➡ Low catalyst charge (0.1 mol% to 50 ppm)
- ➡ Up to 18200 TON and 1250 h⁻¹ TOF values

Scheme 1. Different types of cooperative bimetallic activation of organic molecules (top, dashed and dotted lines refers to activated/cleaved bond in the substrate and non-covalent interactions, respectively) and Mn(I) precursor used for catalytic intermolecular amine-borane dehydrogenation (bottom).

with the interaction of bimetallic frustrated Lewis pairs (FLPs) with dihydrogen,⁹ acetylene,^{9c} amine-boranes¹⁰ or formic acid.¹¹ Conceptually related intermolecular activation of CO_2

^a LCC-CNRS, Université de Toulouse, CNRS, UPS, 205 route de Narbonne, 31077 Toulouse Cedex 4, France. E-mail: yves.canac@lcc-toulouse.fr, dmitry.valyaev@lcc-toulouse.fr

^b A. N. Nesmeyanov Institute of Organoelement Compounds (INEOS), Russian Academy of Sciences, 28/1 Vavilov str., GSP-1, B-334, Moscow, 119334, Russia. E-mail: h-bond@ineos.ac.ru, shu@ineos.ac.ru

[†] Electronic Supplementary Information (ESI) available: Complete experimental procedures, details of DFT calculations, original IR and NMR spectra and kinetic profiles for H_2 evolution. CCDC 2262301 and 2262302 contain the supplementary crystallographic data for this paper. See DOI: 10.1039/x0xx00000x



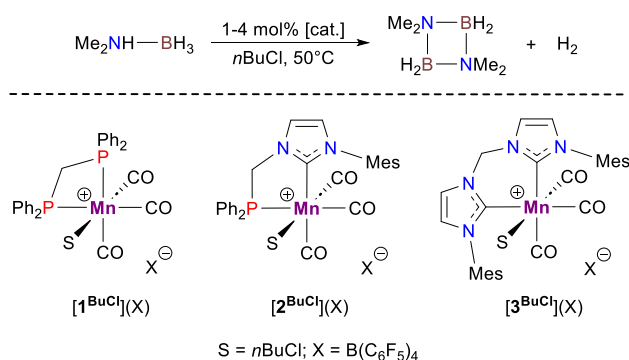
and epoxide by a radical pair arisen from the spontaneous homolytic cleavage of Fe–Al bond in the bimetallic complex prior to the interaction with a substrate was also recently reported.¹² Despite remarkable results already achieved in the area of homogeneous catalysis exploiting bimetallic cooperation, in most cases either quite sophisticated binuclear transition metal complexes (Scheme 1, (a–b))^{3–7} or carefully selected combination of two monometallic species (Scheme 1, (c))¹⁰ were employed. In this contribution, we provide experimental and theoretical evidence for a novel type of *intermolecular* bimetallic cooperativity using Lewis acidic and hydride components (Scheme 1, (d)) generated *in situ* from a single mononuclear metal precursor, halide abstractor and bifunctional substrate. Beyond the apparent simplicity of this approach, its potential usefulness was illustrated by the development of a convenient procedure for dehydrogenation of various amine-boranes catalyzed by air-stable Mn(I) bis(NHC) complex (Scheme 1, bottom) showing in particular state-of-the-art performance for H₂ production from Me₂NHBH₃ (DMAB) largely surpassing all known 3d metal catalysts.

Results and discussion

Discovery and optimization of amine-boranes dehydrogenation catalyzed by Mn(I) complexes *fac*-[(CO)₃(L–L')MnBr] (L, L' = phosphine, NHC).

In a frame of our project dealing with Mn(I) organometallic chemistry relevant to homogeneous catalysis, we have unexpectedly observed that cationic complex [1^{BuCl}]⁺ (Scheme 2) obtained by reaction of the corresponding hydride **1^H** with [Ph₃C](B(C₆F₅)₄) in *n*BuCl was capable to catalyze DMAB dehydrogenation at 50°C to produce H₂ with TOF *ca.* 0.6 h^{–1}. Further studies revealed that parent cationic species [2^{BuCl}]⁺ and [3^{BuCl}]⁺, in which Ph₂P moieties are progressively replaced with more donating *N*-heterocyclic carbene (NHC) fragments, were much more active affording TOF of 9 h^{–1} and 143 h^{–1}, respectively. Encouraged by the latter result being much superior to previously known Mn-based catalysts for this substrate (TOF 0.7–11 h^{–1}),¹⁵ we proceeded to further optimization study.

Looking for a more convenient source of cationic Mn(I) species we first prepared the corresponding MeCN complex



Scheme 2. DMAB dehydrogenation catalyzed by cationic Mn(I) complexes [1–3^{BuCl}](B(C₆F₅)₄)

Table 1. Optimization of DMAB dehydrogenation catalyzed by bis(NHC) Mn(I) complexes^a DOI: 10.1039/D3SC05356C

No	Pre-catalyst	Solv.	Additive	Time, h	TON ^b	TOF ^c , h ^{–1}
1	[3 ^{MeCN}](BF ₄)	PhCl	–	26	981	38
2	3 ^{Br}	PhCl	NaBF ₄	69	902	13
3	3 ^{Br}	PhCl	NaBPh ₄	3.9	1000	259
4	3 ^{Br}	PhCl	NaB(C ₆ F ₅) ₄	4.1	1000	244
5	3 ^{Br}	PhF	NaBPh ₄	6.7	1000	149
6	3 ^{Br}	THF	NaBPh ₄	26	1000	38
7 ^d	3 ^{Br}	DCM	NaBPh ₄	11	100	9
8 ^e	3 ^{Br}	PhCl	NaBPh ₄	4.0	1000	256
9	3 ^{Br}	PhCl	–	118	535	5
10	3 ^H	PhCl	–	69	253	4

^a DMAB (1.5 mmol), 0.1 mol% of pre-catalyst, 1.0 mol% of sodium salt, 2 mL of solvent in a closed vessel at 50°C. ^b Estimated from the pressure changes due to H₂ release under constant volume conditions. ^c TOF values were calculated including 10–20 min induction period required for catalyst activation. ^d 1 mol% of 3^{Br} and 10 mol% of NaBPh₄ at 30°C. ^e Reaction in the presence of 250 equivalents of mercury.

[3^{MeCN}](BF₄) from AgBF₄ and readily available bromide precursor 3^{Br}.¹⁶ This compound was isolated in 85% yield and fully characterized including single crystal X-ray diffraction (Figure S1). While this compound showed a very low activity in *n*BuCl, the use of more chemically inert chlorinated solvent such as PhCl allowed to get almost quantitative DMAB conversion at only 0.1 mol% catalyst charge (Table 1, entry 1). Gratifyingly, the catalyst can be also generated *in situ* from 3^{Br} and NaBF₄ (entry 2) even if its activity was lower than for the isolated [3^{MeCN}](BF₄). The application of sodium salts with non-coordinating anions boosted the catalyst performance (entries 3–4) being now better than for initially tested complex [3^{BuCl}]⁺ in *n*BuCl (*vide supra*). Solvent screening revealed that PhF provided slightly inferior results (entry 5), whereas the use of coordinating THF led to a serious drop of reaction rate (entry 6). The reaction can even slowly proceed in dichloromethane at 30°C (entry 7) albeit ten times higher catalyst loading was required in this case. The addition of mercury did not alter dehydrogenation process (entry 8) thus ruling out well-known catalysis of amine-borane dehydrogenation by metal nanoparticles.^{17,18} Finally, it was observed that neutral 3^{Br} and 3^H without any additives displayed only modest catalytic activity (entries 9–10).

Then we focused on the evaluation of catalytic performance for this system (Table 2). At 60°C the reaction rate is significantly accelerated (entry 1) and catalyst charge may be decreased down to 50 ppm resulting in TON and TOF values of 16221, and 661 h^{–1}, respectively (entries 2–4). Surprisingly, we have noticed that the reaction was even faster in dark providing TON of 18242 at 50 ppm charge of 3^{Br} (entry 5) probably preventing photo-induced catalyst decomposition. Background DMAB dehydrogenation in the presence of NaBPh₄ under these conditions was not observed at all (entry 6). Remarkably, the catalytic performance for this substrate is more than 50 times higher than those previously obtained with 3d metal catalysts (20–330 TONs)^{15,19} especially considering that for the most of them the activation by strong bases (*n*BuLi, *t*BuOK)^{19a,19e–f} or UV-light^{15b–c,19c,19g} was required. The results obtained for catalyst 3^{Br}



Table 2. Dehydrogenation of various amine-boranes catalyzed by bis(NHC) Mn(I) complex **3^{Br}**^a

No	Substrate	3^{Br} , mol%	Time, h	H ₂ , eq. ^{b,c}	TON (TOF, h ⁻¹) ^{b,c}
1	DMAB	0.1	2.1	>0.99	1000 (476)
2	DMAB	0.02	4.8	>0.99	5000 (1058)
3	DMAB	0.01	8.7	>0.99	10000 (1157)
4	DMAB	0.005	24.6	0.81	16221 (661)
5	DMAB	0.005 ^d	14.4	0.91	18242 (1267)
6	DMAB	–	60	<0.01 ^e	–
7	<i>t</i> BuNH ₂ BH ₃	0.1 ^d	48.6	1.53	1527 (31)
8	<i>t</i> BuNH ₂ BH ₃	–	60	0.36 ^e	–
9	MeNH ₂ BH ₃	0.1 ^d	28.4	1.34	1343 (47)
10	MeNH ₂ BH ₃	–	60	0.2 ^e	–
11	NH ₃ BH ₃	0.1 ^d	60	0.61	611 (10)
12	NH ₃ BH ₃	–	60	0.07 ^e	–

^a Amine-borane (0.8–1.5 mmol), 0.5–1.0 mol% of NaBPh₄, 2 mL of PhCl in a sealed vessel at 60°C. ^b Average from two independent runs. ^c Estimated from the pressure changes due to H₂ release under constant volume conditions and ¹¹B NMR spectra of the crude products. ^d In dark. ^e Background dehydrogenation experiments were carried out in the presence of 1.0 mol% of NaBPh₄ under strictly identical conditions to those of Mn-catalyzed process.

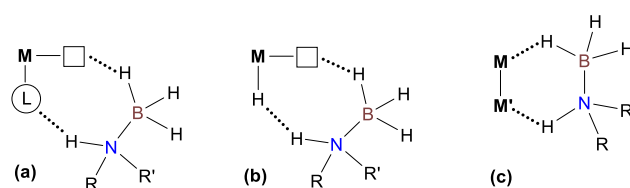
also surpass significantly the TON values obtained for noble metal derivatives (up to 2240 TONs),²⁰ *s*-, *p*- and *f*-block metal complexes (up to 485 TONs)^{21–25} as well as FLP-based systems (up to 500 TONs).²⁶ The only comparable precedent in terms of productivity was reported for Ru(acac)₃/oleylamine combination (TON 15000),²⁷ however the reaction rate in this case was much slower (TOF 78 h⁻¹ at 60°C).

We have found that our system is also suitable for amine-boranes with higher hydrogen content being relevant to hydrogen storage materials.²⁸ Preliminary results without any additional optimization showed that *t*BuNH₂BH₃ can release *ca.* 1.53 equivalents of H₂ with only 0.1 mol% catalyst charge (entry 7). While this substrate can be slowly dehydrogenated under these conditions without any catalyst (entry 8), Mn-catalyzed reaction was much faster to give *ca.* 1.3 equivalents of hydrogen after 10 h (TOF 130 h⁻¹ for this period) followed by a more sluggish process releasing further 0.2 equivalents in *ca.* 40 h (Figure S13). To the best of our knowledge, this value represents the best result ever obtained for this substrate among all other metal complexes.^{10,23b,25a,29} ¹¹B NMR analysis of the crude reaction mixture (Figure S15) revealed the presence of substituted borazine [tBuNBH]₃, cyclic trimer [tBuNHBH₂]₃ and oligomers [tBu₃NHBH₂]_n as main dehydrogenation products. We suppose that the drop of reaction rate after evolution of the first equivalent of hydrogen was caused by more difficult uptake of partially dehydrogenated products by our catalytic system. Dehydrogenation of MeNH₂BH₃ (entry 9) was found to be slightly slower than in case of *t*BuNH₂BH₃ (TOF 123 h⁻¹ for 10 h period) and less efficient in terms of produced H₂ amount (1.2 equivalents, Figure S13), probably due to lower solubility of this substrate in PhCl and extensive formation of insoluble polymeric products [MeNHBH₂]_n. However, the catalytic efficiency obtained in this case (TON 1343) is competitive with a majority of known 3d metal catalysts (TON 20–250)³⁰ and remains inferior only to highly active Co-based complexes (TON

up to 5000).³¹ Finally, the reaction for NH₃BH₃ afforded 0.61 equivalents of H₂ in 60 h (entry 11) leading to the formation of insoluble polymer [NH₂BH₂]_n. The TON value was estimated in a range of about 500–550 considering background substrate dehydrogenation process (entry 12). However, despite slow reaction kinetics and low amount of produced dihydrogen compared to the best catalytic systems based on first row transition metal complexes³² or purely organic molecules³³ working at 1–5 mol% catalyst charge (1.7–2.5 equiv. of H₂ per NH₃BH₃), these numbers are still superior in terms of overall performance to previously reported Mn-based catalysts (TON *ca.* 50–70).³⁴ Considering the remarkable progress recently achieved in formic acid dehydrogenation using Mn(I) complexes,³⁵ our results further highlight a privileged position of this metal in the future design of sustainable homogeneous catalysts for H₂ production.

Spectroscopic and kinetic studies of the reaction mechanism for DMAB dehydrogenation catalyzed by Mn(I) complex *fac*-[(CO)₃(bis(NHC))MnBr] (**3^{Br}**).

Next, we turned attention to a deeper understanding of this catalytic system, as all conventional known mechanisms for transition metal-catalyzed amine-borane dehydrogenation³⁶ based on either metal-ligand cooperation (Scheme 3, (a)), reactivity of coordinatively unsaturated hydrides (Scheme 3, (b)) or bimetallic activation (Scheme 3, (c)) are *a priori* inappropriate in our case. Firstly regarding possible metal-ligand cooperation, it should be noted that the non-innocent character of dppe³⁷ and NHC-phosphine³⁸ ligands by the deprotonation of the CH₂ bridge in the corresponding Mn(I) bromide complexes may be only observed in the presence of strong base, which is not required in the present case. Furthermore, no evidence for the cooperative behavior of bis(NHC) ligand incorporated into the most active catalyst was reported so far, which thus permit us to exclude the path (a). Then, despite extensive applications of different manganese bis(NHC) complexes in hydrosilylation,^{16a,39} electrochemical CO₂ reduction,^{16b,40} hydrogenation⁴¹ and hydrogen-borrowing processes⁴² systematically involving hydride intermediates *fac*-[(CO)₃(bis(NHC))MnH], the dissociation of a CO ligand in such species has been never proved experimentally. While, the formation of the dicarbonyl complex *fac*-[(CO)₂(η²-H₂)(bis(NHC))MnH] from H₂ and tricarbonyl hydride precursor was recently proposed in Mn-catalyzed ester hydrogenation mechanism,^{42a} the calculated barrier for CO-to-H₂ substitution of 38.5 kcal mol⁻¹ seems to be too high for our reaction conditions thus making the path (b) very unlikely (*vide infra*). Finally, the bimetallic activation pathway⁴³ (Scheme 3, (c)) can be also ruled out because of insufficient reducing ability of



Scheme 3. An overview of main known approaches for amine-boranes dehydrogenation catalyzed by transition metal complexes.



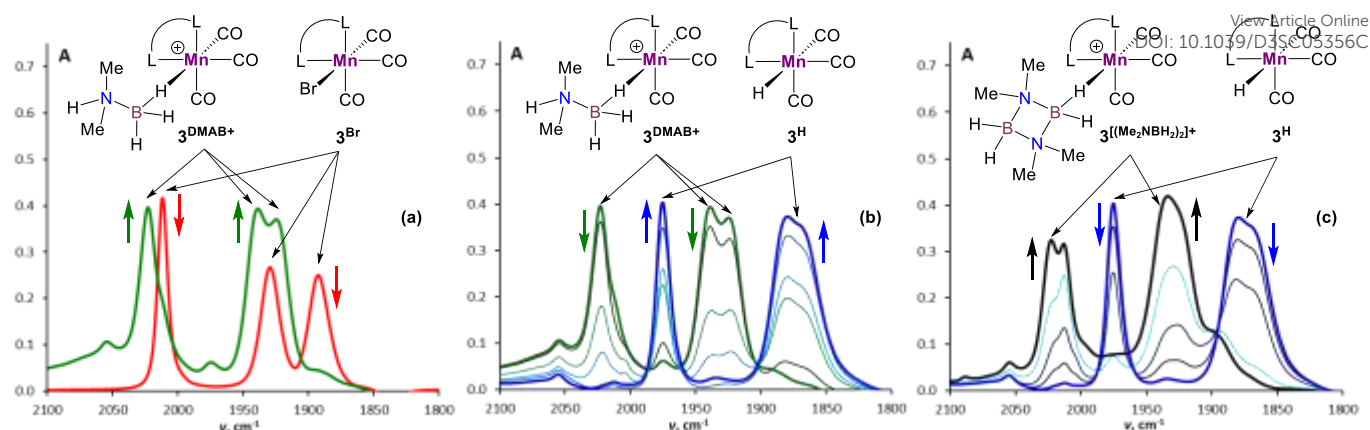


Figure 1. IR spectroscopy monitoring in ν_{CO} range for DMAB dehydrogenation in the presence of $\mathbf{3}^{\text{Br}}$ (3.3 mol.%) and NaBPh₄ (16.5 mol.%) in CH₂Cl₂ at ca. 30 °C (L–L = bis(NHC), c (DMAB) = 0.30 M, l = 0.01 cm). (a) IR spectra of initial $\mathbf{3}^{\text{Br}}$ solution (red) and reaction mixture after 2 min upon DMAB addition (green). (b) IR spectra between 2 min (green) and 20 min (blue) of reaction time. (c) IR spectra between 20 min (blue) and 40 min (black) of reaction time.

amine-boranes to form Mn(0) derivatives from $\mathbf{3}^{\text{Br}}$ and apparent impossibility of metal-metal bond formation for [(CO)₃(bis(NHC))Mn] radical due to steric hindrance.^{40b}

We have started our mechanistic investigations from operando spectroscopic monitoring of the catalytic process in CH₂Cl₂. This solvent was chosen instead of PhCl because of slower reaction kinetics (Table 1), its full transparency in ν_{CO} region and the availability of deuterated version for NMR studies. Similar trends were also observed in PhCl (Figure S19) albeit full set of spectroscopic data for reaction intermediates cannot be obtained in this solvent (see the ESI for details). The analysis of the IR spectra of $\mathbf{3}^{\text{Br}}$ /NaBPh₄/DMAB solution in ν_{CO} region (Figure 1) revealed an initial transformation of the starting bromide into the cationic species [$\mathbf{3}^{\text{DMAB}}$](BPh₄) with coordinated substrate (Figure 1, (a)). Subsequent evolution of the latter into the hydride $\mathbf{3}^{\text{H}}$ (Figure 1, (b)) is consistent with induction period observed by volumetric H₂ evolution studies (*vide infra*). The concomitant conversion of DMAB into the

dimer [Me₂NBH₂]₂ was evident from characteristic changes in ν_{BH} region (Figure S18). After full DMAB consumption $\mathbf{3}^{\text{H}}$ rapidly decayed giving a mixture of neutral chloride compound $\mathbf{3}^{\text{Cl}}$ and cationic complex [$\mathbf{3}^{\text{Me}_2\text{NBH}_2}_2$](BPh₄) bearing coordinated [Me₂NBH₂]₂ ligand (Figure 1, (c), see Figure S17 for ν_{CO} bands deconvolution). ¹¹B NMR monitoring of the reaction mixture in CD₂Cl₂ (Figure S23) showed the appearance of the characteristic signal of Me₂N=BH₂ at δ_{B} 37.4 ppm, being consistent with “off-metal” dimerization mechanism for the formation of the final product.³⁶ The ¹H NMR spectra (Figure S21) confirmed the presence of the hydride complex $\mathbf{3}^{\text{H}}$ at δ_{H} –7.04 ppm and revealed additionally a broad signal at δ_{H} –3.38 ppm. We were able to retrieve a full set of NMR data for this intermediate (see the ESI) being attributed to a cationic Mn(I) σ -borane complex [$\mathbf{3}^{\text{DMAB}}$](BPh₄).

In order to confirm this attribution we prepared the model Mn(I) cationic complex [$\mathbf{3}^{\text{Me}_3\text{NBH}_3}$](BPh₄) from Me₃NBH₃ unreactive towards dehydrogenation, $\mathbf{3}^{\text{Br}}$ and NaBPh₄. Its structure elucidated from X-ray diffraction (Figure 2) features a η^1 -BH coordination mode previously observed in half-sandwich Mn(I) analogues.⁴⁴ The BH₃ moiety in NMR spectra of [$\mathbf{3}^{\text{Me}_3\text{NBH}_3}$](BPh₄) appears as broad signals at δ_{B} –11.9 ppm and δ_{H} –3.30 ppm. The latter value matches well with that observed during the NMR mechanistic investigation clearly indicating the participation of such species in the catalytic process. According to IR and NMR data all transformations occurring in catalytic DMAB dehydrogenation involved only tricarbonyl Mn(I) complexes and we did not find any spectroscopic evidence for the formation of neutral dicarbonyl hydride species *fac*-[(CO)₂(DMAB)(bis(NHC))MnH] essential for the realization of the route (b) depicted in Scheme 3.

The kinetic studies revealed [pseudo]zero order for the substrate (Figure S27) and first order for catalyst concentration (Figure S28). The variation in the amount of NaBPh₄ (0.125–8 mol%) showed virtually no influence on the reaction rate (Figure S29), thus permitting to rule out the occurrence of conceptually similar DMAB dehydrogenation process with operating *via* a Na⁺/Mn–H couple. While reversible coordination of sodium cation with DMAB cannot be excluded, we suppose that this

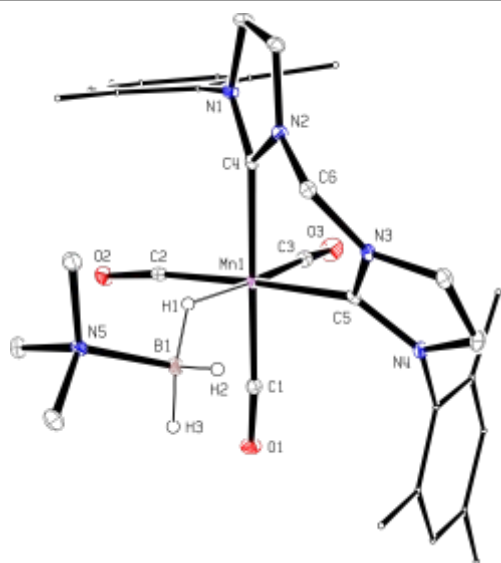


Figure 2. Molecular geometry of complex [$\mathbf{3}^{\text{Me}_3\text{NBH}_3}$](BPh₄) (20% probability ellipsoids, Mes groups represented as wireframe, most hydrogen atoms, BPh₄[–] anion and CH₂Cl₂ solvate molecule are not shown).



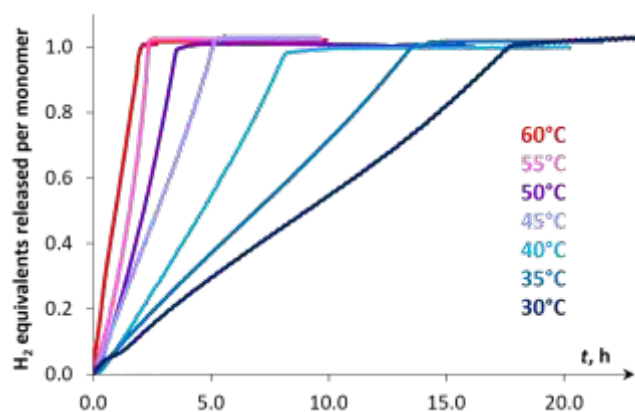


Figure 3. Hydrogen evolution kinetic curves for DMAB dehydrogenation in PhCl catalyzed by 3^{Br} (0.1 mol%) and NaBPh_4 (1 mol%) at various temperatures. Initial parts of curves corresponding to the induction period (10–20 min) are not shown.

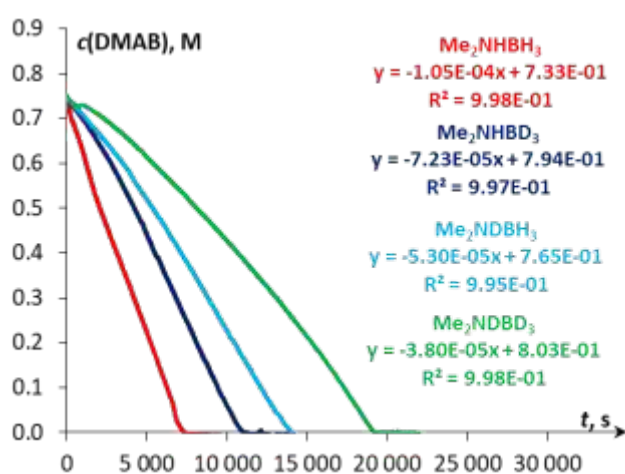


Figure 4. $c(\text{DMAB})$ vs. time plots for initial reaction rates determination of Me_2NHBH_3 , Me_2NHBD_3 , Me_2NDBH_3 and Me_2NDBD_3 ($c_0 = 0.75$ M) dehydrogenation catalyzed by 3^{Br} (0.1 mol%) in the presence of NaBPh_4 (1.0 mol%) in PhCl at 60°C.

interaction is too weak to activate the substrate towards deprotonation with the Mn(I) hydride complex 3^{H} (*vide infra*). Variable temperature experiments in the 30–60°C range (Figure 3) allowed to estimate the activation enthalpy $\Delta H^\ddagger = 14.5 \pm 0.4$ kcal mol $^{-1}$ (Figure S26, Table S6) being typical for proton transfer to transition metal hydrides.⁴⁵ The detailed description of proposed kinetic model is provided in the ESI. Finally, kinetic isotope effects ($k_{\text{H}}/k_{\text{D}}$, Figure 4) measured at 60°C for Me_2NHBD_3 (1.5 ± 0.1), Me_2NDBH_3 (2.1 ± 0.1) and Me_2NDBD_3 (2.9 ± 0.1) are consistent with an involvement of B–H and N–H bond cleavage in the rate determining step.^{32a,32c} These data taken together with spectroscopic results showing the implication of cationic and hydride Mn(I) species in the catalytic process allowed to propose an unconventional intermolecular DMAB activation, which was then studied by theoretical means.

Theoretical investigation of DMAB dehydrogenation catalyzed by Mn(I) complex *fac*-[(CO) $_3$ (bis(NHC))MnBr] (3^{Br}).

Computational modelling of the catalytic system showed that each of monometallic species 3^+ and 3^{H} interacts with DMAB (Figure 5) *via* B–H coordination and dihydrogen bonding, respectively. However, activation barriers for the subsequent

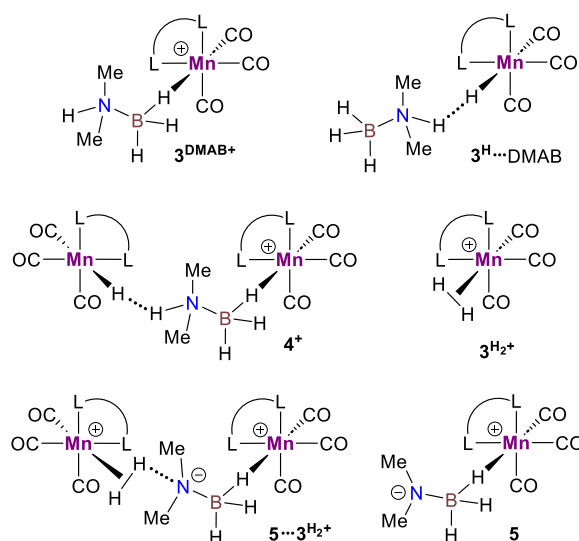
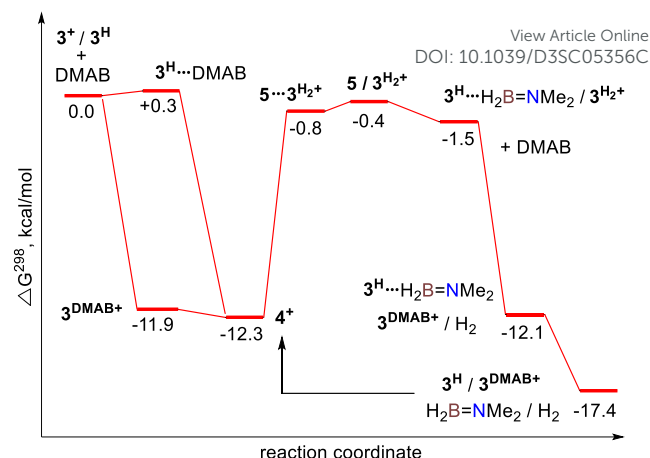


Figure 5. Calculated Gibbs energy profile for DMAB dehydrogenation catalyzed by $3^+/3^{\text{H}}$ couple at $\omega\text{B97XD}/\text{def2-TZVP}$ level in toluene (dihydrogen bond interactions are indicated as dotted lines, non-interacting molecules are separated by slash) and structures of the key intermediates (bottom).

hydride and proton transfer steps in these intermediates [$3^{\text{DMAB}}]^+$ and $3^{\text{H}}\cdots\text{DMAB}$ exceed 30–40 kcal/mol and no stabilization of the resulting products was evidenced by DFT calculations (Figures S31 and S33). In contrast, proton transfer becomes feasible in the most thermodynamically stable adduct 4^+ , in which two metal fragments are bridged by DMAB molecule. Both N–H (1.040 Å) and B–H (1.264 Å) bonds of coordinated DMAB moiety in 4^+ are slightly longer than those in the corresponding mononuclear species $3^{\text{H}}\cdots\text{DMAB}$ (1.028 Å) and $3^{\text{DMAB}+}$ (1.258 Å) thus being consistent with higher extent of substrate activation. This process leads initially to the formation of bimetallic intermediate $5\cdots 3^{\text{H}_2+}$ composed of the cationic dihydrogen complex [$3^{\text{H}_2}]^+$ associated with the zwitter-ionic species **5** by hydrogen bonding (2.283 Å) undergoing then the dissociation to the individual components. Importantly, metal-coordinated B–H bond distance in complexes $5\cdots 3^{\text{H}_2+}$ and **5** becomes elongated by 0.093 and 0.234 Å, respectively, relative to that in 4^+ with a concomitant shortening of Mn–H distance by 0.056 and 0.109 Å, respectively. These data are in agreement



with the occurrence of a progressive hydride transfer in the sequence $5 \cdots 3^{H_2+} \rightarrow 5 \rightarrow 3^H \cdots BH_2 = NMe_2$. Finally, the essentially barrierless loss of H_2 and $Me_2N=BH_2$ from $[3^{H_2}]^+$ and $3^H \cdots BH_2 = NMe_2$, respectively regenerate $3^+/3^H$ couple thus exhibiting a curious interconversion of both metal species after each catalytic turnover. The key role of bimetallic adducts 4^+ and $5 \cdots 3^{H_2+}$ in DMAB activation process provides an additional argument to consider this reaction mechanism as a viable intermolecular bimetallic cooperation (Scheme 1, (d)).

Proposed catalytic cycle for DMAB dehydrogenation catalyzed by Mn(I) complex *fac*-[(CO)₃(bis(NHC))MnBr] (3^{Br}).

The catalytic cycle for DMAB dehydrogenation emerging from the results of the spectroscopic and kinetic studies combined with the DFT calculations is shown in Scheme 4. The activation steps (Scheme 4, top) include bromide abstraction from 3^{Br} with $NaBPh_4$ in the presence of substrate affording the cationic intermediate $[3^{DMAB}](BPh_4)$. Its slow deprotonation by the traces of amine and/or water followed by hydride transfer presumably leads to the initial accumulation of 3^H essential for the catalytic process. Indeed, addition of isolated 3^H to $3^{Br}/NaBPh_4/DMAB$ mixture resulted in immediate H_2 evolution without any induction period (Figure 6). Interestingly, the formation of ternary adduct $[4](BPh_4)$ is favorable in terms of Gibbs energy regardless large entropy effect. This intermediate undergoes a sequence of N-H/B-H bond cleavage steps ultimately affording 3^H , $Me_2N=BH_2$, and $[3^{H_2}](BPh_4)$, which rapidly exchanges the H_2 ligand for DMAB thus restoring initial $[3^{DMAB}](BPh_4)$. First order kinetics on metal, spectroscopic detection of 3^H as a resting state and KIE values are consistent with low steady-state concentration of the cation $[3^{DMAB}](BPh_4)$ in the reaction mixture and its deprotonation by 3^H via the formation of $[4](BPh_4)$ as the rate-determining step. Thus, the

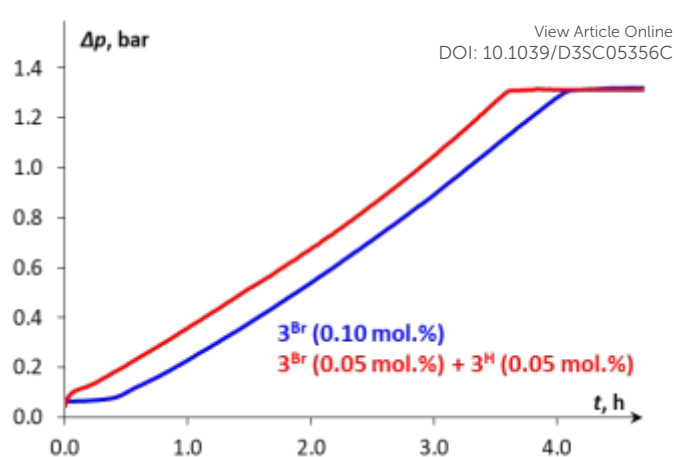
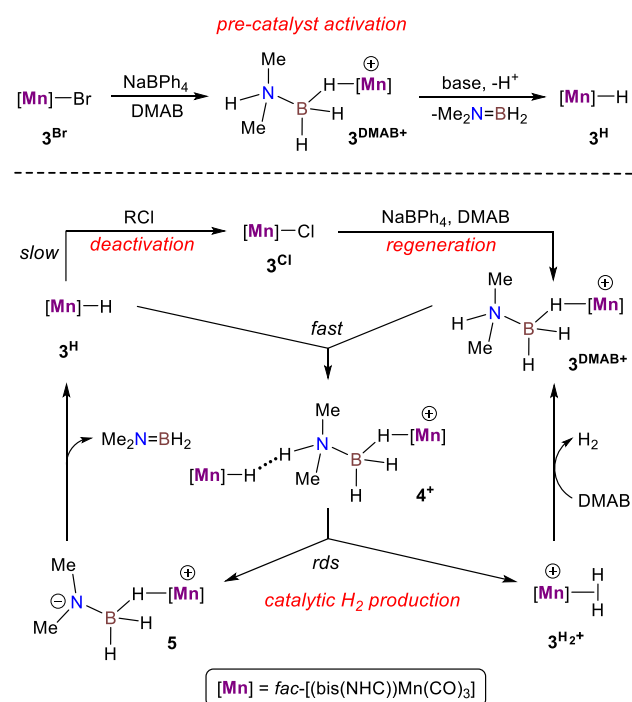


Figure 6. Kinetic profile (Δp vs. time) for DMAB dehydrogenation in PhCl at 50°C catalyzed either by 0.1 mol% 3^{Br} or by the mixture of 3^{Br} (0.05 mol%) and 3^H (0.05 mol%) in the presence of $NaBPh_4$ (1 mol%).

overall reaction rate depends on variable 3^{DMAB+} concentration, while 3^H concentration remains constant giving the effective reaction rate law $r_3 = k_{eff}[3^{DMAB+}]$ (see Scheme S2 and the associated text in the ESI for a complete kinetic model). For this reason, despite the simultaneous presence of two metal complexes (3^H and 3^{DMAB+}), first reaction order in overall concentration of manganese species was actually observed. In this context, beneficial NHC effect in the series of Mn(I) complexes with bidentate ligands (Scheme 2) can be rationalized by a synergy between a better stabilization of the cationic species and a higher basicity of the corresponding hydrides. Very importantly, complex 3^H may be observed in the reaction mixture *uniquely in the presence of amine-borane substrate*, whereas isolated hydride decomposes rapidly in PhCl at 50–60°C to form mainly chloride derivative 3^{Cl} . We suppose that such counter-intuitive survival of 3^H in a variety of chlorinated solvents ($nBuCl$, PhCl, CH_2Cl_2) may be explained by faster dehydrogenation kinetics vs. chlorination and efficient regeneration of cationic complex $[3^{DMAB}]^+$ from 3^{Cl} by the excess of halide abstractor (Scheme 4) thus explaining the observed trend in the catalytic activity in PhCl $\gg nBuCl > CH_2Cl_2$ row and the overall robustness of our catalytic system resulting in high TON values.

Conclusions

We have evidenced by spectroscopic, kinetic and theoretical means a new type of intermolecular bimetallic cooperativity between hydride and cationic species clearly illustrating that a simple mononuclear metal halide precursor can be at the origin of two catalytically active species actually doing two complementary jobs for one price. The potential of this approach for homogeneous catalysis was demonstrated by the development of practical and efficient system for amine-boranes dehydrogenation based on air-stable bis(NHC) Mn(I) complex and $NaBPh_4$, being capable to work at low catalyst charge and provide unprecedented level of TONs for Me_2NHBH_3 and $tBuNH_2BH_3$ substrates. Our results also show that



Scheme 4. Proposed mechanism for DMAB dehydrogenation catalyzed by bis(NHC) Mn(I) complex 3^{Br}



nucleophilic metal hydrides can successfully operate in chlorinated solvents if the catalytic process is faster than decomposition thus allowing to shake up a longstanding paradigm about their incompatibility. Taking into account a plethora of known monometallic halide complexes bearing strongly donor ligands, we hope that this contribution will boost the interest to broader use of intermolecular bimetallic cooperation phenomena in organometallic chemistry and homogeneous catalysis.

Data availability

All relevant experimental data and details of DFT calculations are provided in the ESI. Deposition numbers 2262301 (for $[3^{\text{MeCN}}](\text{BF}_4)$) and 2262302 (for $[3^{\text{Me}_3\text{NBH}_3}](\text{BPh}_4)$) contain the supplementary crystallographic data for this paper.

Author Contributions

O.A.F., N.V.B., E.S.S., Y.C. and D.A.V. planned and guided the research project. E.S.O. and D.A.V. acquired the research funding. E.S.G. carried out the main experimental work and performed initial data analysis. E.S.O. and S.A.K. participated in IR mechanistic investigations. O.A.F. performed the DFT calculations. L.V. and D.A.V. carried out X-ray diffraction experiments. E.S.G., E.S.O., O.A.F., N.V.B., E.S.S., Y.C. and D.A.V. participated in manuscript preparation. All authors have approved the final version of the manuscript.

Conflicts of interest

There are no conflicts to declare.

Acknowledgements

The work was financially supported by the Russian Science Foundation (grant no. 22-73-00072, spectroscopic mechanistic studies) and by the CNRS. E.S.G. is grateful to the French Embassy in Moscow for a joint PhD fellowship (Vernadski program). Computational studies were performed using HPC resources from CALMIP (grant no. P18038). Spectroscopic data were partially collected using the equipment of the Center for Molecular Composition Studies of INEOS RAS with the support from the Ministry of Science and Higher Education of the Russian Federation (contract no. 075-03-2023-642). We thank Dr. Noël Lugan and Dr. Olivier Baslé for helpful discussions.

References

- (a) L. Liu and A. Corma, *Chem. Rev.*, 2023, **123**, 4855–4933; (b) L. Liu and A. Corma, *Chem. Rev.*, 2018, **118**, 4981–5079.
- R. H. Holm, P. Kennepohl and E. I. Solomon, *Chem. Rev.*, 1996, **96**, 2239–2314.
- Selected reviews: (a) A. C. Ghosh, C. Duboc and M. Gennari, *Coord. Chem. Rev.*, 2021, **428**, 213606; (b) C.-H. Wang and S. DeBeer, *Chem. Soc. Rev.*, 2021, **50**, 8743–8761; (c) C. Ferousi, S. H. Majer, I. M. DiMucci and K. M. Lancaster, *Chem. Rev.*, 2020, **120**, 5252–5307; (d) J. Serrano-Plana, I. Garcia-Bosch, A. Company and M. Costas, *Acc. Chem. Res.*, 2015, **48**, 2397–2406; (e) M. D. Kärkäs, O. Verho, E. V. Johnston and B. Åkermark, *Chem. Rev.*, 2014, **114**, 11863–12001; (f) M. Costas, K. Chen and L. Que Jr., *Coord. Chem. Rev.*, 2000, **200**–**202**, 517–544.
- (a) C. Uyeda and C. M. Farley, *Acc. Chem. Res.*, 2021, **54**, 3710–3719; (b) I. G. Powers and C. Uyeda, *ACS Catal.*, 2017, **7**, 936–958; (c) D. C. Powers and T. Ritter, *Acc. Chem. Res.*, 2012, **45**, 840–850.
- J. Bauer, H. Braunschweig and R. D. Dewhurst, *Chem. Rev.*, 2012, **112**, 4329–4346.
- (a) R. Govindarajan, S. Deolka and J. R. Khusnutdinova, *Chem. Sci.*, 2022, **13**, 14008–14031; (b) N. P. Mankad, *Chem. Commun.*, 2018, **54**, 1291–1302; (c) L. H. Gade, *Angew. Chem. Int. Ed.*, 2000, **39**, 2658–2678.
- (a) H.-C. Yu, S. M. Islam and N. P. Mankad, *ACS Catal.*, 2020, **10**, 3670–3675; (b) L.-J. Cheng and N. P. Mankad, *J. Am. Chem. Soc.*, 2019, **141**, 3710–3716; (c) M. K. Karunananda and N. P. Mankad, *J. Am. Chem. Soc.*, 2015, **137**, 14598–14601; (d) S. R. Parmelee, T. J. Mazzacano, Y. Zhu, N. P. Mankad and J. A. Keith, *ACS Catal.*, 2015, **5**, 3689–3699; (e) T. J. Mazzacano and N. P. Mankad, *J. Am. Chem. Soc.*, 2013, **135**, 17258–17261.
- (a) M. Navarro, J. J. Moreno, M. Pérez-Jiménez and J. Campos, *Chem. Commun.*, 2022, **58**, 11220–11235; (b) B. Chatterjee, W.-C. Chang, S. Jena and C. Werlé, *ACS Catal.*, 2020, **10**, 14024–14055.
- (a) N. Hidalgo, F. de la Cruz-Martínez, M. T. Martín, M. C. Nicasio and J. Campos, *Chem. Commun.*, 2022, **58**, 9144–9147; (b) N. Hidalgo, J. J. Moreno, M. Pérez-Jiménez, C. Maya, J. López-Serrano and J. Campos, *Chem. Eur. J.*, 2020, **26**, 5982–5993; (c) J. Campos, *J. Am. Chem. Soc.*, 2017, **139**, 2944–2947.
- E. S. Osipova, E. S. Gulyaeva, E. I. Gutsul, V. A. Kirikina, A. A. Pavlov, Yu. V. Nelyubina, A. Rossin, M. Peruzzini, L. M. Epstein, N. V. Belkova, O. A. Filippov and E. S. Shubina, *Chem. Sci.*, 2021, **12**, 3682–3692.
- E. S. Osipova, D. V. Sedlova, E. I. Gutsul, Yu. V. Nelyubina, P. V. Dorovatovskii, L. M. Epstein, O. A. Filippov, E. S. Shubina and N. V. Belkova, *Organometallics*, 2023, **42**, 2651–2660.
- S. Sinhababu, M. R. Radzhabov, J. Telser and N. P. Mankad, *J. Am. Chem. Soc.*, 2022, **144**, 3210–3221.
- E. S. Osipova, E. S. Gulyaeva, N. V. Kireev, S. A. Kovalenko, C. Bijani, Y. Canac, D. A. Valyaev, O. A. Filippov, N. V. Belkova and E. S. Shubina, *Chem. Commun.*, 2022, **58**, 5017–5020.
- E. S. Osipova, S. A. Kovalenko, E. S. Gulyaeva, N. V. Kireev, A. A. Pavlov, O. A. Filippov, A. A. Danshina, D. A. Valyaev, Y. Canac, E. S. Shubina and N. V. Belkova, *Molecules*, 2023, **28**, 3368.
- (a) H. R. Sharpe, A. M. Geer, T. J. Blundell, F. R. Hastings, M. W. Fay, G. A. Rance, W. Lewis, A. J. Blake and D. L. Kays, *Catal. Sci. Technol.*, 2017, **8**, 229–235; (b) S. Muhammad, S. Moncho, E. N. Brothers and A. A. Bengali, *Chem. Commun.*, 2014, **50**, 5874–5877; (c) T. Kakizawa, Y. Kawano, K. Naganeyama and M. Shimoi, *Chem. Lett.*, 2011, **40**, 171–173.
- Previously described synthesis of 3^{Br} (ref. 16) was reoptimized using weak base (K_2CO_3) in DMF at 120°C to give target product in 82% yield avoiding the generation of free bis(NHC) with strong bases. (a) Y. Yang, Z. Zhang, X. Chang, Y.-Q. Zhang, R.-Z. Liao and L. Duan, *Inorg. Chem.*, 2020, **59**, 10234–10242; (b) M. Pinto, S. Friães, F. Franco, J. Lloret-Fillol and B. Royo, *ChemCatChem* **2018**, **10**, 2734–2740.
- W.-W. Zhan, Q.-L. Zhu and Q. Xu, *ACS Catal.*, 2016, **6**, 6892–6905.
- For the formation of Mn/Hg intermetallic compounds, see: (a) Z. Moser and C. Guminski, *JPE*, 1993, **14**, 726–733; (b) J. F. de Wet, *Angew. Chem.*, 1955, **67**, 208; (c) O. Prelinger, *Monatsh. Chem.* 1893, **14**, 353–370.



- 19 (a) E. A. LaPierre, B. O. Patrick and I. Manners, *J. Am. Chem. Soc.*, 2019, **141**, 20009–20015; (b) C. Lichtenberg, L. Viciu, M. Adelhardt, J. Sutter, K. Meyer, B. de Bruin and H. Grützmacher, *Angew. Chem. Int. Ed.*, 2015, **54**, 5766–5771; (c) J. R. Vance, A. Schäfer, A. P. M. Robertson, K. Lee, J. Turner, G. R. Whittell and I. Manners, *J. Am. Chem. Soc.*, 2014, **136**, 3048–3064; (d) T.-P. Lin and J. C. Peters, *J. Am. Chem. Soc.*, 2013, **135**, 15310–15313; (e) M. Vogt, B. de Bruin, H. Berke, M. Trincado and H. Grützmacher, *Chem. Sci.*, 2011, **2**, 723–727; (f) M. E. Sloan, A. Staubitz, T. J. Clark, C. A. Russell, G. C. Lloyd-Jones and I. Manners, *J. Am. Chem. Soc.*, 2010, **132**, 3831–3841; (g) Y. Kawano, M. Uruichi, M. Shimoi, S. Taki, T. Kawaguchi, T. Kakizawa and H. Ogino, *J. Am. Chem. Soc.*, 2009, **131**, 14946–14957.
- 20 For noble metal catalysts for DMAB dehydrogenation working at 0.5 mol% charge or below, see: (a) S. Pal, S. Kusumoto and K. Nozaki, *Organometallics*, 2018, **37**, 906–914; (b) E. H. Kwan, H. Ogawa and M. A. Yamashita, *ChemCatChem*, 2017, **9**, 2457–2462; (c) E. U. Barin, M. Masjedi and S. Özkur, *Materials*, 2015, **8**, 3155–3167; (d) H. C. Johnson, E. M. Leitao, G. R. Whittell, I. Manners, G. C. Lloyd-Jones and A. S. Weller, *J. Am. Chem. Soc.*, 2014, **136**, 9078–9093; (e) D. F. Schreiber, C. O'Connor, C. Grave, Y. Ortin, H. Müller-Bunz and A. D. Phillips, *ACS Catal.*, 2012, **2**, 2505–2511; (f) R. Dallanegra, A. P. M. Robertson, A. B. Chaplin, I. Manners and A. S. Weller, *Chem. Commun.*, 2011, **47**, 3763–3765; (g) A. Friedrich, M. Drees and S. Schneider, *Chem. Eur. J.*, 2009, **15**, 10339–10342.
- 21 For reviews on amine-boranes dehydrogenation using catalysts based on main-group elements, see: (a) D. H. A. Boom, A. R. Jupp and J. C. Sootweg, *Chem. Eur. J.*, 2019, **25**, 9133–9152; (b) R. L. Melen, *Chem. Soc. Rev.*, 2016, **45**, 775–788.
- 22 Alkaline metal catalysts: (a) R. McLellan, A. R. Kennedy, R. E. Mulvey, S. A. Orr and S. D. Robertson, *Chem. Eur. J.*, 2017, **23**, 16853–16861; (b) P. Bellham, M. S. Hill and G. Kociok-Köhn, *Dalton Trans.*, 2015, **44**, 12078–12081.
- 23 Alkaline earth metal catalysts: (a) L. Wirtz, K. Y. Ghulam, B. Morgenstern and A. Schäfer, *ChemCatChem*, 2022, **14**, e202201007; (b) L. Wirtz, W. Haider, V. Huch, M. Zimmer and A. Schäfer, *Chem. Eur. J.*, 2020, **26**, 6176–6184; (c) A. C. A. Ried, L. J. Taylor, A. M. Geer, H. E. L. Williams, W. Lewis, A. J. Blake and D. L. Kays, *Chem. Eur. J.*, 2019, **25**, 6840–6846; (d) X. Zheng, J. Huang, Y. Yao and X. Xu, *Chem. Commun.*, 2019, **55**, 9152–9155; (e) D. J. Liptrot, M. S. Hill, M. F. Mahon and D. J. MacDougall, *Chem. Eur. J.*, 2010, **16**, 8508–8515.
- 24 Group 3 metal catalysts: (a) P. Xu and X. Xu, *Organometallics*, 2019, **38**, 3212–3217; (b) E. Lu, Y. Yuan, Y. Chen and W. Xia, *ACS Catal.*, 2013, **3**, 521–524; (c) H. J. Cowley, M. S. Holt, R. L. Melen, J. M. Rawson and D. S. Wright, *Chem. Commun.*, 2011, **47**, 2682–2684. (d) M. S. Hill, G. Kociok-Köhn and T. P. Robinson, *Chem. Commun.*, 2010, **46**, 7587–7589.
- 25 Lanthanide- and actinide-based catalysts: (a) V. A. Kirikina, A. A. Kissel, A. N. Selikhov, Yu. V. Nelyubina, O. A. Filippov, N. V. Belkova, A. A. Trifonov and E. S. Shubina, *Chem. Commun.*, 2022, **58**, 859–862; (b) K. A. Erickson and J. L. Kiplinger, *ACS Catal.*, 2017, **7**, 4276–4280; (c) P. Cui, T. P. Spaniol, L. Maron and J. Okuda, *Chem. Eur. J.*, 2013, **19**, 13437–13444.
- 26 (a) M. Boudjelel, E. D. Sosa Carrizo, S. Mallet-Ladeira, S. Massou, K. Miqueu, G. Bouhadir and D. Bourissou, *ACS Catal.*, 2018, **8**, 4459–4464; (b) C. Appelt, J. C. Sootweg, K. Lammertsma and W. Uhl, *Angew. Chem. Int. Ed.*, 2013, **52**, 4256–4259; (c) A. M. Chapman, M. F. Haddow and D. F. Wass, *J. Am. Chem. Soc.*, 2011, **133**, 8826–8829.
- 27 S. Duman, M. Masjedi and S. Özkur, *J. Mol. Catal. A*, 2016, **411**, 9–18.
- 28 (a) A. Staubitz, A. P. M. Robertson and I. Manners, *Chem. Rev.*, 2010, **110**, 4079–4124; (b) C. W. Hamilton, R. T. Baker, A. Staubitz and I. Manners, *Chem. Soc. Rev.*, 2009, **38**, 279–293.
- 29 (a) K. A. Erickson, J. P. W. Stelmach, N. T. Mucha and R. Waterman, *Organometallics*, 2015, **34**, 4693–4699; (b) D. García-Vivó, E. Huergo, M. A. Ruiz, R. Travieso-Puente, *Eur. J. Inorg. Chem.*, 2013, **2013**, 4998–5008.
- 30 (a) F. Anke, S. Boye, A. Spannenberg, A. Lederer, D. Heller and T. Beweries, *Chem. Eur. J.*, 2020, **26**, 7889–7899; (b) T. M. Maier, S. Sandl, I. G. Shenderovich, A. J. von Wangelin, J. J. Weigand and R. Wolf, *Chem. Eur. J.*, 2019, **25**, 238–245; (c) T. Jurca, T. Dellermann, N. E. Stubbs, D. A. Resendiz-Lara, G. R. Whittell and I. Manners, *Chem. Sci.*, 2018, **9**, 3360–3366; (d) F. Anke, D. Han, M. Klahn, A. Spannenberg and T. Beweries, *Dalton Trans.*, 2017, **46**, 6843–6847; (e) C. Lichtenberg, M. Adelhardt, T. L. Gianetti, K. Meyer, B. de Bruin and H. Grützmacher, *ACS Catal.*, 2015, **5**, 6230–6240.
- 31 T. M. Boyd, K. A. Andrea, K. Baston, A. Johnson, D. E. Ryan and A. S. Weller, *Chem. Commun.*, 2020, **56**, 482–485.
- 32 (a) P. Bhattacharya, J. A. Krause and H. Guan, *J. Am. Chem. Soc.*, 2014, **136**, 11153–11161; (b) R. T. Baker, J. C. Gordon, C. W. Hamilton, N. J. Henson, P.-H. Lin, S. Maguire, M. Murugesu, B. L. Scott and N. C. Smythe, *J. Am. Chem. Soc.*, 2012, **134**, 5598–5609; (c) R. J. Keaton, J. M. Blacquire and R. T. Baker, *J. Am. Chem. Soc.*, 2007, **129**, 1844–1845.
- 33 (a) M. Hasenbeck, J. Becker and U. Gellrich, *Angew. Chem. Int. Ed.*, 2020, **59**, 1590–1594; (b) Z. Mo, A. Rit, J. Campos, E. L. Kolychev and S. Aldridge, *J. Am. Chem. Soc.*, 2016, **138**, 3306–3309; (c) Z. Lu, L. Schweighauser, H. Hausmann and H. A. Wegner, *Angew. Chem. Int. Ed.*, 2015, **54**, 15556–15559; (d) W. C. Ewing, A. Marchione, D. W. Himmelberger, P. J. Carroll and L. G. Sneddon, *J. Am. Chem. Soc.*, 2011, **133**, 17093–17099.
- 34 (a) K. Sarkar, K. Das, A. Kundu, D. Adhikari and B. Maji, *ACS Catal.*, 2021, **11**, 2786–2794; (b) M. Gediga, C. M. Feil, S. H. Schlindwein, J. Bender, M. Nieger and D. Gudat, *Chem. Eur. J.*, 2017, **23**, 11560–11569.
- 35 (a) D. Wei, X. Shi, P. Sponholz, H. Junge and M. Beller, *ACS Cent. Sci.*, 2022, **8**, 1457–1463; (b) D. Wei, R. Sang, P. Sponholz, H. Junge and M. Beller, *Nat. Energy*, 2022, **7**, 438–447; (c) A. Léval, A. Agapova, C. Steinlechner, E. Alberico, H. Junge and M. Beller, *Green Chem.*, 2020, **22**, 913–920.
- 36 (a) A. Rossin and M. Peruzzini, *Chem. Rev.*, 2016, **116**, 8848–8872; (b) S. Bhunya, T. Malakar, G. Ganguly and A. Paul, *ACS Catal.*, 2016, **6**, 7907–7934.
- 37 N. V. Kireev, O. A. Filippov, E. S. Gulyaeva, E. S. Shubina, L. Vendier, Y. Canac, J.-B. Sortais, N. Lugan and D. A. Valyaev, *Chem. Commun.*, 2020, **56**, 2139–2142.
- 38 R. Buhaibeh, O. A. Filippov, A. Bruneau-Voisine, J. Willot, C. Duhayon, D. A. Valyaev, N. Lugan, Y. Canac and J.-B. Sortais, *Angew. Chem. Int. Ed.*, 2019, **58**, 6727–6731.
- 39 (a) S. C. A. Sousa, S. Realista and B. Royo, *Adv. Synth. Catal.*, 2020, **362**, 2437–2443; (b) B. Royo, C. J. Carrasco, S. C. A. Sousa and M. F. Pinto, *ChemCatChem*, 2019, **11**, 3839–3843.
- 40 (a) S. Fernández, F. Franco, M. Martínez Belmonte, S. Friães, B. Royo, J. M. Luis and J. Lloret-Fillol, *ACS Catal.*, 2023, **13**, 10375–10385; (b) F. Franco, F. Pinto, M. B. Royo and J. Lloret-Fillol, *Angew. Chem. Int. Ed.*, 2018, **57**, 4603–4606.
- 41 (a) N. F. Both, A. Spannenberg, H. Jiao, K. Junge and M. Beller, *Angew. Chem. Int. Ed.*, 2023, **62**, e202307987; (b) K. Azouzi, L. Pedussaut, R. Pointis, A. Bonfiglio, R. Kumari Riddhi, C. Duhayon, S. Bastin and J.-B. Sortais, *Organometallics*, 2023, **42**, 1832–1838.
- 42 (a) K. Ganguly, A. Mandal and S. Kundu, *ACS Catal.*, 2022, **12**, 12444–12457; (b) X.-B. Lan, Z. Ye, J. Liu, M. Huang, Y. Shao, X. Cai, Y. Liu and Z. Ke, *ChemSusChem*, 2020, **13**, 2557–2563; (c) X.-B. Lan, Z. Ye, M. Huang, J. Liu, Y. Liu and Z. Ke, *Org. Lett.*, 2019, **21**, 8065–8070; (d) M. Huang, Y. Li, Y. Li, J. Liu, S. Shu, Y. Liu and Z. Ke, *Chem. Commun.*, 2019, **55**, 6213–6216.
- 43 (a) K. Lindénau, N. Jannsen, M. Rippke, H. Al Hamwi, C. Selle, H.-J. Drexler, A. Spannenberg, M. Sawall, K. Neymeyr, D.



View Article Online

DOI: 10.1039/D3SC05356C

- Heller, F. Reiß and T. Beweries, *Catal. Sci. Technol.*, 2021, **11**, 4034–4050; (b) C. Cesari, B. Berti, F. Calcagno, C. Lucarelli, M. Garavelli, R. Mazzoni, I. Rivalta and S. Zacchini, *Organometallics*, 2021, **40**, 2724–2735; (c) M. Trose, M. Reiß, F. Reiß, F. Anke, A. Spannenberg, S. Boye, A. Lederer, P. Arndt and T. Beweries, *Dalton Trans.*, 2018, **47**, 12858–12862; (d) T. Miyazaki, Y. Tanabe, M. Yuki, Y. Miyake and Y. Nishibayashi, *Organometallics*, 2011, **30**, 2394–2404.
- 44 (a) T. Yasue, Y. Kawano and M. Shimoi, *Angew. Chem. Int. Ed.*, 2003, **42**, 1727–1730; (b) T. Kakizawa, Y. Kawano and M. Shimoi, *Organometallics*, 2001, **20**, 3211–3213.
- 45 (a) N. V. Belkova, L. M. Epstein, O. A. Filippov and E. S. Shubina, *Chem. Rev.*, 2016, **116**, 8545–8587; (b) N. V. Belkova, L. M. Epstein and E. S. Shubina, *Eur. J. Inorg. Chem.*, 2010, **2010**, 3555–3565.

